

# A Precambrian microcontinent in the Indian Ocean

Trond H. Torsvik<sup>1,2,3,4,5\*</sup>, Hans Amundsen<sup>6</sup>, Ebbe H. Hartz<sup>1,7</sup>, Fernando Corfu<sup>4</sup>, Nick Kuznir<sup>8</sup>, Carmen Gaina<sup>1,2,4</sup>, Pavel V. Doubrovine<sup>1,2</sup>, Bernhard Steinberger<sup>9,1,2</sup>, Lewis D. Ashwal<sup>5</sup> and Bjørn Jamtveit<sup>1</sup>

**The Laccadives-Chagos Ridge and Southern Mascarene Plateau in the north-central and western Indian Ocean, respectively, are thought to be volcanic chains formed above the Réunion mantle plume<sup>1</sup>, over the past ~65.5 million years<sup>2,3</sup>. Here we use U-Pb dating to analyse the ages of zircon xenocrysts found within young lavas on the island of Mauritius, part of the Southern Mascarene plateau. We find that the zircons are either Palaeoproterozoic (more than 1971 million years old) or Neoproterozoic (between 660 and 840 million years old). We propose that the zircons were assimilated from ancient fragments of continental lithosphere beneath Mauritius, and were brought to the surface by plume-related lavas. We use gravity data inversion to map crustal thickness and find that Mauritius forms part of a contiguous block of anomalously thick crust that extends in an arc northwards to the Seychelles. Using plate tectonic reconstructions, we show that Mauritius and the adjacent Mascarene Plateau may overlie a Precambrian microcontinent that we call Mauritia. On the basis of reinterpretation of marine geophysical data<sup>31</sup> we propose that Mauritia was separated from Madagascar and fragmented into a ribbon-like configuration by a series of mid-ocean ridge jumps during the opening of the Mascarene ocean basin between 83.5 and 61 million years ago.**

---

<sup>1</sup> Physics of Geological Processes, University of Oslo, 0316 Oslo, Norway; <sup>2</sup>Center of Advanced Study, Norwegian Academy of Science and Letters, 0271 Oslo, Norway; <sup>3</sup>Geodynamics, NGU, N-7491 Trondheim, Norway; <sup>4</sup>Geosciences, University of Oslo, Postbox 1047 Blindern, 0316 Oslo, Norway; <sup>5</sup>School of Geosciences, University of Witwatersrand, WITS 2050, South Africa; <sup>6</sup>EPX, Jacob Aalls Gate 44b, N-0364 Oslo, Norway; <sup>7</sup>Det norske oljeselskap, Postboks 2070 Vika, 0125 Oslo, Norway; <sup>8</sup>Department of Earth and Ocean Sciences, University of Liverpool, Liverpool, L69 BX, UK.; <sup>9</sup>Helmholtz Centre Potsdam, GFZ German Research Centre for Geosciences, Heinrich-Mann-Allee 18/19, 14473 Potsdam, Germany. \*e-mail: [t.h.torsvik@geo.uio.no](mailto:t.h.torsvik@geo.uio.no). Present address: Centre for Earth Evolution and Dynamics, University of Oslo, 0316 Oslo, Norway.

## **We suggest that the plume-related magmatic deposits have since covered Mauritia and potentially other continental fragments.**

Intra-plate magmatic activity is commonly attributed to melting associated with an upwelling mantle plume. Mantle plumes may also trigger continental breakup and continental fragments may hence be placed along an oceanic hotspot track. A dozen of hotspot volcanoes — including Réunion (Fig. 1) — and most reconstructed large igneous provinces (LIPs) since Pangea assembly (~320 Myr BP) are thought to be sourced by deep plumes from the edges of the two large low shear-wave velocity provinces at the core-mantle boundary<sup>4,5</sup>. Recent volcanics erupted at the island of Réunion show geochemical signatures indicative of homogeneous mantle domains<sup>6</sup>, whereas lavas from Mauritius show much more heterogeneous isotopic compositions. Mauritian basalts<sup>7,8</sup> are divided into Older (8.9-5.5 Myr BP), Intermediate (3.5-1.9 Myr BP) and Younger (1-0.03 Myr BP) Series that are geochemically and isotopically distinct, and have been proposed to form from a variety of source components, including variably enriched and depleted peridotites, as well as ‘pods’ of more enriched material, possibly pyroxenites and/or eclogites<sup>8-10</sup>.

Here we report Precambrian zircons recovered from basaltic beach sands on Mauritius, 900 km distant from the nearest continental crust (Madagascar). Some twenty zircon grains were recovered from two basaltic sand samples from the northwest (Sample E04-1) and southeast (Sample MBS1) coast of Mauritius. The use of sand samples avoids potential contamination from rock crushing apparatus. The zircons are generally subhedral to anhedral, show diversity in shape and presence of inclusions, and range in size from 50 to 300  $\mu\text{m}$ . The zircons were analysed for U and Pb isotopes by TIMS (Fig. 2, Supplementary Table S1). Sample E04-1 from the Intermediate Series yielded fifteen zircon grains; six were selected for analysis. Sample MBS1 from the Older Series had fewer zircons and two were used for age determination. Most results are somewhat discordant (Fig. 2), but all data indicate a Proterozoic age of the grains. The oldest grain has a minimum age of 1971 Myr. Three grains yield ages between 1400 and 900 Myr. Four grains are Neoproterozoic, two grains showing discordant  $^{207}\text{Pb}/^{206}\text{Pb}$  ages of ~840 Myr, one grain yielding a concordant age of 790 Myr, and another grain showing reversely discordant age of ~690-660 Myr (Supplementary Table S1). Their presence in exclusively basaltic detritus suggests that they were brought up by mafic magmas that assimilated underlying sialic crust, likely at relatively shallow levels. There is no clear cut geochemical or isotopic signature of continental crust in the Mauritian basalts, although some of their variability in  $\epsilon_{\text{Nd}}$  values (3.9-6.1; refs 8,9) could indicate variable crustal contamination. We suggest that a crustal signature need not be detectable in basaltic lavas that carry xenocrystic zircons. Although small amounts of zircon have been found as crystallization products in young oceanic

mafic volcanics and intrusives<sup>11,12</sup>, older xenocrystic zircons have been reliably documented only from oceanic gabbros drilled at the mid-Atlantic ridge<sup>13</sup>. The young Mid-Atlantic ridge gabbros that contain old xenocrystic zircons have lower Zr concentrations<sup>13</sup> (mean ~20 ppm) than Mauritian basalts<sup>8</sup> (mean ~145 ppm), and also lack geochemical indicators of continental crust assimilation.

To identify regions in the northwest Indian Ocean that may be underlain by continental crust, we determined crustal thicknesses by gravity anomaly inversion incorporating a lithosphere thermal gravity anomaly correction<sup>14</sup>. The gravity inversion predicts contiguous crust of thickness >25–30 km beneath the Seychelles and northern Mascarenes, which extends southwards towards Mauritius (Fig. 1). Sensitivity tests (Supplementary Fig. S1) show that predicted crustal thicknesses from gravity inversion under the Seychelles, Mascarenes, Mauritius, Laccadives, Maldives and Chagos are not significantly dependent on breakup and ocean age isochrons used to determine the lithosphere thermal gravity anomaly correction. Crustal thickness determined from gravity inversion for the Seychelles is consistent with wide-angle seismic studies<sup>15</sup> where crustal thicknesses of 32 km and velocity structure are interpreted as continental. On the conjugate Indian margin, the Laccadives, Maldives and Chagos also appear to be underlain by contiguous crust of thickness >25–30 km. Seismic Moho depths (~24 km) beneath the Laccadives<sup>16</sup> and crustal thicknesses from Chagos (up to 27 km) obtained from gravity modelling<sup>17</sup> are similar to our thickness estimates. These regions of thick crust identified by gravity inversion are surrounded by oceanic crust of thickness typically <5–10 km within the Mascarene Basin, between the Seychelles-Mascarenes and Laccadives-Maldives-Chagos ridge, and to the east of the Laccadives-Maldives-Chagos ridge. Crustal thickness patterns, oceanic fracture zones revealed by the free air gravity anomaly and plate reconstructions all strongly suggest that Chagos was originally joined to the Mascarene plateau (Fig. 1 and Supplementary Figs S1 and S2). It should be noted that crustal thickness mapping using gravity inversion cannot distinguish thinned continental crust from anomalously thick ocean crust.

Our new U-Pb data demonstrate that the proposed Palaeoproterozoic continental crust ( $\geq 1971$  Ma) beneath Mauritius underwent reworking/magmatism during the Neoproterozoic (840–660 Myr BP). This continental signature is recognized in surface exposures from both Madagascar and India, and Neoproterozoic arc-related magmatism (800–700 Myr BP) is well known in the Seychelles and NW India<sup>18–20</sup>. We place the post-750 Myr BP position of Mauritius between Southern India and Madagascar (Fig. 3 and Supplementary Fig. S3) and further propose that thinned continental crust beneath the Laxmi Ridge<sup>15</sup> is of Neoproterozoic age, and was originally juxtaposed to the Seychelles and the Malani province in India (Supplementary Fig. S3). We name the proposed sub-volcanic crust of Mauritius, and potentially other continental fragments from the Southern Mascarene Plateau (for

example, parts of Saya de Malha, Nazareth and Cargados-Carjos Banks) and from the conjugate Indian margin (Laccadives and Chagos) as Mauritia.

Mauritian continental lithosphere was thinned, fragmented and concealed during Cretaceous-Cenozoic times. A Late Cretaceous LIP event (~91-84 Myr BP), which we attribute to the Marion plume, first blanketed most of Madagascar<sup>21</sup> (horizontal stripes in Fig. 3a) parts of SW India<sup>22</sup> and probably also Mauritia with flood basalts. The plume center was probably located near the southern tip of Madagascar (Fig. 3a). The Mascarene Basin opened shortly thereafter, separating India from Madagascar and the African plate. In our model, Mauritius and other parts of Mauritia were attached to Madagascar, but were gradually transferred to the Indian plate as a NE-SW ribbon-like structure that parallels the Mahanoro-Wilshaw and Mauritius fracture zones (Fig. 1) through a system of SW propagating ridge-jumps, adding more crust to the Indian plate (Supplementary Figs S4, S5). We model three major ridge jumps (80, 73.6 and 70 Myr BP; Fig. 3b), and by 70 Myr BP all Mauritian fragments were transferred to the Indian plate. Following the peak of Deccan magmatism (65.5 Myr BP), seafloor spreading was initiated between the Laxmi Ridge and the Seychelles (62-63 Myr; refs 23,24) with seafloor spreading still ongoing in the Mascarene Basin. Shortly after 61 Myr BP (chron C27), the Reunion plume was located beneath the SW margin of India, which probably assisted a major NE ridge jump that led to the termination of seafloor spreading in the Mascarene Basin. By 56 Myr BP, the Mauritian fragments (except Laccadives) and the Seychelles became part of the African plate (Supplementary Fig. S5). Thereafter, the Reunion Plume was beneath the slowly moving African plate (~2 cm yr<sup>-1</sup>). A SW ridge jump around 41 Myr BP resulted in Chagos breaking away from the Mascarene Plateau and becoming part of the Indian plate (Fig. 3C and Supplementary Fig. S5). Continuing volcanic activity later modified the Southern Mascarene Plateau.

Coincidence of a plume track and continental fragments may result if the plume assists in breaking off these fragments. Palaeomagnetic data corrected for true polar wander (Supplementary Fig. S6a) from Deccan volcanics and deep-sea drilling LEG 115 Sites 715 and 707 (Fig. 1) are compatible with a moving hotspot model<sup>25</sup>, and this, together with the general volcanic ridge geometry and age progression, strongly supports a deeply-sourced plume beneath Réunion. Our plate model<sup>25</sup>, based on five hotspot tracks (including Réunion), does, however, predict a hotspot track somewhat west of the main chain of volcanic islands and submarine plateaus. But even if the Réunion track is not used to construct a global model, the predicted track is remarkably similar (Supplementary Fig. S7 and Fig. 1 inset map). The trend of the Réunion chain is therefore close to what is expected from a global plate motion model, but the predicted track is ~100 km westward along the Southern Mascarene Plateau. This region is located within a ~350 km-wide zone limited by two major fracture zones<sup>26</sup> that separate lithosphere of different age (Supplementary Fig. S7) and

thickness. Mauritius and the Nazareth Bank are located at or near the Mauritius fault zone, probably as a result of plume material travelling up-slope and eastwards towards younger and thinner oceanic lithosphere<sup>27</sup>.

Basalt compositions along the Réunion hotspot chain vary with time toward less MORB-like (less depleted) isotopic signatures<sup>28</sup>. This trend is best understood by examining isotopic compositions versus distance from the spreading ridge at the time of eruption (Supplementary Fig. S6b,c). During eruption of the Deccan Traps, the Réunion plume was located beneath India and more than 500 km from an active spreading ridge (Supplementary Fig. S6b), but prominent ridge-jumps leading to the end of seafloor spreading in the Mascarene Basin (Fig. 3b) and Chagos splitting off from the Mascarene Plateau (Fig. 3c) were a direct result of a vigorous Réunion plume. This led to short periods of plume-ridge interactions (55–40 Myr BP) and more MORB-like basalt compositions. With time, the Réunion plume probably became less vigorous and ridge-plume distance increased systematically for the past 40 Myr. All existing plate reconstructions assume that Chagos belonged to the Indian plate at ~50 Myr BP (Site 713, Fig. 1). We show, however, that Chagos was joined to the Mascarenes and that the Réunion plume was beneath the African plate at this time. Consequently, the Réunion plume remained directly beneath the Indian plate only for ~10 Myr (65–55 Myr BP). This has implications for modelling plate motions based on hotspot tracks, and we further advise against using volcanics from Site 707 (64.1 Myr BP) when constructing such models, since it was erupted close to the ridge and ~500 km from the Réunion plume conduit (Supplementary Fig. S6b).

The Seychelles has long been considered as a geological peculiarity, and represents a Precambrian continental fragment left behind after Pangea break-up. We show here for the first time that likewise Mauritius may be underlain by continental lithosphere material and propose that thinned continental crust imaged seismically beneath the Laxmi Ridge<sup>15</sup> on the conjugate Indian margin, as well as the crust of Mauritia, partly formed through Neoproterozoic arc-related intrusive activity, as in the Seychelles<sup>20</sup>. These proposed continental fragments gradually rifted and were separated from the Indian and African plates, respectively, by a series of Late Cretaceous-Early Cenozoic plate boundary relocations, probably triggered by both the Marion and Réunion plumes. The Indian Ocean could be littered with continental fragments, but the extent of continental crust remains speculative because these fragments have been obscured by hotspot-related volcanism. It is puzzling, but probably coincidental, that absolute plate motions were such that, subsequent to fragmentation, the Réunion hotspot trail followed continental fragments along the Southern Mascarene Plateau for the past 50 Myr. We show that the Réunion hotspot trail is close to what is expected from absolute plate motion models, but it is likely that lithospheric heterogeneities, including two major fracture zones,

fossil (Cretaceous) ridges and continental lithospheric fragments, combined with plume-ridge interactions, had a subsidiary control on the distribution of surface volcanics. Critical to furthering our tale of lost continents are deep drilling, acquisition of high quality seismic refraction data, and rigorous search for zircon xenocrysts, coupled with geochemistry, geochronology and plate reconstructions.

## **METHODS**

Great care was taken to eliminate the risk of contamination when collecting material for U-Pb analyses, and two samples from NW and SE Mauritius (Supplementary Table S1) were collected from beaches adjacent to eroding columnar basalts. Sampling beach sand eliminates the need for rock crushing and thus the chance for contaminating the sample with zircons from previously processed samples. Beach sands were collected from trenches dug to the base of beach foresets, where heavy minerals are concentrated, and sieved and concentrated on location using entirely new equipment. The samples were then sealed until further processing at the University of Oslo. The sand concentrates were passed through 250  $\mu\text{m}$  disposable sieves and the finer grained fraction further enriched with a Frantz magnetic separator and heavy liquid (methylene iodide), before the final handpicking in alcohol under a binocular microscope. All the material used in the separation was either new, or carefully disassembled and cleaned in an ultrasonic bath followed by blasting with a compressed air jet. A general, independent, test for the cleanliness of the procedure in this lab is provided periodically when samples of volcanic rocks and mafic dykes subjected to crushing and mineral separation fail to yield even a single zircon grain. The selected zircons were cleaned in acid, and dissolved in Krogh-type dissolution bombs after addition of a mixed  $^{205}\text{Pb}/^{235}\text{U}$  spike. Solutions larger than a few  $\mu\text{g}$  were passed through anion exchange columns to isolate U and Pb. The isotopic measurements were done in a MAT262 mass spectrometer in static mode with multiple Faraday cups or by peak jumping with a secondary electron multiplier, depending on signal strength. Fractionation factors of 0.1 %  $\text{amu}^{-1}$  for Pb and 0.12 %  $\text{amu}^{-1}$  for U were determined by daily measurements of the NBS 982 Pb and U500 standards. Given the nature of the problem being investigated, it was not deemed necessary to abrade the zircons. Analytical procedures are detailed in ref. 29.

Satellite-derived gravity anomaly and bathymetry data were used to derive the mantle residual gravity anomaly, and subsequently inverted in the 3D spectral domain to give Moho depth<sup>14</sup>. A thermal gravity anomaly correction was implemented and corrections were made for both sedimentary thickness and crustal volcanic addition due to decompression melting during continental break-up lithosphere thinning and sea-floor spreading. The gravity inversion uses a reference crustal

thickness of 36 km, a continental breakup age of 65 Myr BP and a crustal basement density of 2850 kg m<sup>-3</sup> (see Supplementary Figs S1 and S2).

Absolute plate reconstructions use the global moving hotspot (mantle) reference frame of ref. 25. Relative plate kinematics within the Indian Ocean basin is based on interpretations of marine magnetic anomalies and fracture zones (see Supplementary Information). A principal difference between our plate model and previous Indian Ocean plate reconstructions is that we include extra continental fragments and postulate several ridge jumps that led to important plate boundary relocations. The ages of extinct ridges are inferred from the geometry of plate boundaries at different times, interpretation of magnetic anomalies and high asymmetry of crust production within the south westernmost spreading corridor of the Mascarene basin, where much more crust has been accreted to the northeast flank (Supplementary Fig. S4). Based on our new plate model we produced a new seafloor age grid for the Indian Ocean (Supplementary Fig. S7).

Received 10 August 2012; accepted 18 January 2013; published online 24 February 2013

## REFERENCES

1. Richards, M.A., Duncan, R.A. & Courtillot, V.E. Flood basalts and hotspot tracks: plume heads and tails. *Science* **146**, 103-107 (1989).
2. Duncan, R.A. In *Proceedings of the Ocean Drilling Program Scientific Results 115* (eds Duncan, R.A., Backman, J. & Peterson, L.C.) 3-10 (1990).
3. Courtillot, V., Davaille, A., Besse, J. & Stock, J. Three distinct types of hotspot in the Earth's mantle. *Earth Planet. Sci. Lett.* **205**, 295-308 (2003).
4. Burke, K., Steinberger, B., Torsvik, T.H. & Smethurst, M.A. Plume Generation Zones at the margins of Large Low Shear Velocity Provinces on the core–mantle boundary. *Earth Planet. Sci. Lett.* **265**, 49-60 (2008).
5. Torsvik, T.H., Burke, K., Steinberger, B., Webb, S.C. & Ashwal, L.D. Diamonds sourced by plumes from the core mantle boundary. *Nature* **466**, 352-355 (2010).
6. Vlastelic, I., Lewin, E. & Staudacher, T. Th/U and other geochemical evidence for the Réunion plume sampling a less differentiated mantle domain. *Earth Planet. Sci. Lett.* **248**, 379-393 (2006).
7. McDougall, I. & Chamalaun, F.H. Isotopic dating and geomagnetic polarity studies on volcanic rocks from Mauritius, Indian Ocean. *Geol. Soc. Am. Bull.*, **80**, 1419-1442 (1969).

8. Moore, J. *et al.* Evolution of shield-building and rejuvenescent volcanism of Mauritius. *J. Volc. Geothermal Res.* 207, 47-66 (2011).
9. Paul, D., White, W.M. & Blichert-Toft, J. Geochemistry of Mauritius and the origin of rejuvenescent volcanism on oceanic island volcanoes. *Geochem. Geophys. Geosyst.* 6, Q06007 (2005).
10. Paul, D., Kamenetsky, V.S., Hofmann, A.W. & Stracke, A. Compositional diversity among primitive lavas of Mauritius, Indian Ocean: Implications for mantle sources. *J. Volc. Geothermal Res.* **164**, 76-94 (2007).
11. Grimes, C.B. *et al.* Trace element chemistry of zircon from oceanic crust: A method for distinguishing detrital zircon provenance. *Geology* **7**, 643-646 (2007).
12. Simonetti, A., Neal, C.R. In-situ chemical, U-Pb dating, and Hf isotope investigation of megacrystic zircons, Malaita (Solomon Islands): Evidence for multi-stage alkaline magmatic activity beneath the Ontong Java Plateau. *Earth Planet. Sci. Lett.* 295, 251-261 (2010).
13. Pilot, J., Werner, C.D., Haubrich, F. & Baumann, N. Paleozoic and Proterozoic zircons from the Mid-Atlantic Ridge. *Nature* 393, 676-679 (1998).
14. Greenhalgh, E.E. & Kusznir, N.J. Evidence for thin oceanic crust on the extinct Aegir Ridge, Norwegian Basin, NE Atlantic derived from satellite gravity inversion. *Geophys. Res. Lett.* **34**, L06305 (2007).
15. Collier, J.S. *et al.* Factors influencing magmatism during continental breakup: New insights from a wide-angle seismic experiment across the conjugate Seychelles-Indian margins, *J. Geophys. Res.* **114**, B03101 (2009).
16. Chaubey, A.K. *et al.* Analyses of multichannel seismic reflection, gravity and magnetic data along a regional profile across the central-western continental margin of India. *Marine Geology* **182**, 303-323 (2001).
17. Henstock, T.J. & Thompson, P.J. Self-consistent modeling of crustal thickness at Chagos-Laccadive ridge from bathymetry and gravity data. *Earth Planet. Sci. Lett.* **224**, 325-336 (2004).
18. Collins, A.S. & Windley, B.F. The tectonic evolution of Central and Northern Madagascar and its place in the final assembly of Gondwana. *J. Geology* **110**, 325-339 (2002).
19. Ashwal, L.D., Demaiffe, D. & Torsvik, T.H. Petrogenesis of Neoproterozoic granitoids and related rocks from the Seychelles: evidence for an Andean arc origin. *J. Petrology* **43**, 45-83 (2002).



20. Collins, A.S., Kinny, P.D. & Razakamanana, T. Depositional age, provenance and metamorphic age of metasedimentary rocks from southern Madagascar. *Gondwana Research* **21**, 353-361 (2012).
21. Storey, M., Mahoney, J.J. Saunders, A.D., Duncan, R.A., Kelley, S.P. & Coffin, M.F. Timing of hot spot-related volcanism and the break-up of Madagascar and India. *Science* **267**, 852-855 (1995).
22. Torsvik, T.H. *et al.* Late Cretaceous India-Madagascar fit and timing of break-up related magmatism. *Terra Nova* **12**, 220-225 (2000).
23. Collier, J.S. *et al.* Age of Seychelles-India break-up. *Earth Planet. Sci. Lett* **272**, 264-277 (2008).
24. Ganerød, M. *et al.* In *The Formation and Evolution of Africa: A Synopsis of 3.8 Ga of Earth History* (Eds Van Hinsbergen, D.J.J., Buitert, S.J.H., Torsvik, T.H., Gaina, C. & Webb, S.J.) Geological Society London Special Publications **357**, 229-252 (2011).
25. Doubrovine, P.V., Steinberger, B. & Torsvik, T.H. Absolute plate motions in a reference frame defined by moving hotspots in the Pacific, Atlantic and Indian oceans. *J. Geophys. Res.* **117**, B09101 (2012).
26. Lénat, J.-F., Merle, O. & Lespagnol, L. La réunion: An example of channeled hot spot plume. *J. Volc. Geothermal Res.* **184**, 1-13 (2009).
27. Sleep, N.H. Lateral flow and ponding of starting plume material. *J. Geophys. Res.* **102**, 10001-10012 (1997).
28. White, W.M., Cheatham, M.M. & Duncan, R.A. In *Proceedings of the Ocean Drilling Program Scientific results 115* (eds Duncan, R.A., Backman, J. & Peterson, L.C.) 53-61 (1990).
29. Corfu, F. U–Pb age, setting, and tectonic significance of the anorthosite–mangerite–charnockite–granite-suite, Lofoten–Vesterålen, Norway. *J. Petrology* **45**, 1799-1819 (2004).
30. Becker, T.W. & Boschi, L. A comparison of tomographic and geodynamic mantle models. *Geochem. Geophys. Geosyst.* **3**, 1003 (2002).
31. National Geophysical Data Center, National Oceanic and Atmospheric Administrations, US Department of Commerce, <http://ww.ngdc.noaa.gov/mgg/>.

## **Acknowledgements**

We thank E.R. Neuman for discussions, and C. Mac Niocaill for constructive comments. The European Research Council under the European Union's Seventh Framework Programme (FP7/2007-2013) / ERC Advanced Grant Agreement Number 267631 (Beyond Plate Tectonics), the Norwegian Research Council (Topo-4D) and the Centre for Advanced Study are acknowledged for financial support.

## **Author Contributions**

T.H.T., H.A. and B.J. developed the conceptual idea for the study, H.A. and E.H. sampled the Mauritius rocks, F.C. dated the samples, N.K. calculated the crustal thickness map, C.G. and T.H.T. developed detailed reconstructions, P.D. and B.S. developed global plate motion frames, and L.D.A. and B.J. handled geochemical aspects. All authors contributed to discussions and writing of the manuscript.

## **Additional information**

Supplementary information is available in the online version of the paper. Reprints and permissions information is available online at <http://www.nature.com/reprints>. Correspondence and requests for materials should be addressed to T.H.T.

## **Competing financial interests**

The authors declare no competing financial interests.

## FIGURE CAPTIONS

### **Figure 1 | Crustal thickness map based on gravity inversion and the Réunion hotspot chain.**

Circled numbers denote times (Myr) when the Réunion plume<sup>25</sup> was beneath or near Indian (red circle) or African plates. Triangles denote dated sites (see also inset map for ages). The red line is the 1% slow contour in the SMEAN model<sup>30</sup>, approximating the plume generation zone<sup>4,5</sup> at the core-mantle boundary. RR, Rodriguez Ridge. The inset map shows free-air gravity, predicted Réunion track as in the large map but with 95% confidence ellipses and the calculated surface hotspot motion<sup>25</sup> (black line with green circles). The second track (maroon line with black circles) is calculated by excluding the Réunion track when calculating the global mantle reference frame (Supplementary Fig. S7).

### **Figure 2 | U-Pb concordia diagram.**

Data are shown with  $2\sigma$  error ellipses (Supplementary Table S1) surrounded by yellow circles. Corresponding zircon grains are shown in microscope view prior to analysis. The two largest grains, which give concordant to nearly concordant results at ~790 and 680 Myr BP, are ~300  $\mu\text{m}$  long. The two grains from MBS1 were the smallest (~50  $\mu\text{m}$  each).

### **Figure 3 | Late Cretaceous to Eocene plate reconstructions.**

Mantle reference frame<sup>25</sup> with surface location for Réunion (R) and Marion (Ma) hotspots. Mean plate speeds calculated for India (IND) and Africa (AFR). During the opening of the Mascarene Basin (83.5-70 Myr BP), Mauritius (M) and parts of Mauritania were attached to Madagascar but relocated to the Indian plate through three SW-propagating ridge jumps (dashed white extinct ridges, XR). At 61 Myr BP, the Réunion plume assisted a NE-directed ridge jump and the new ridge (Carlsberg) separated Chagos (C) from the Indian plate. At ~41 Myr BP, a SW-directed ridge jump returned Chagos to the Indian plate. SM, Saya de Malha; L, Laccadives.

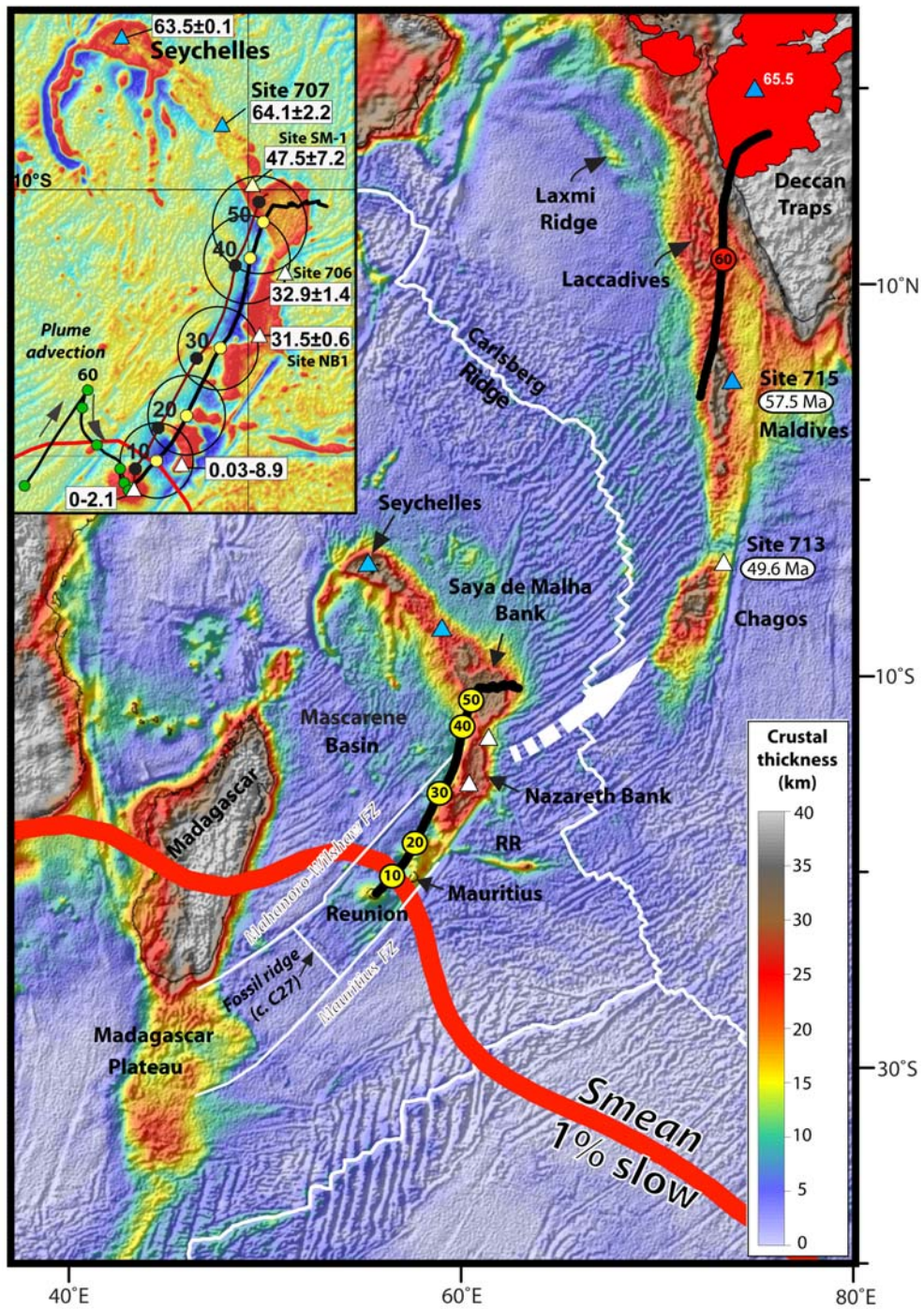
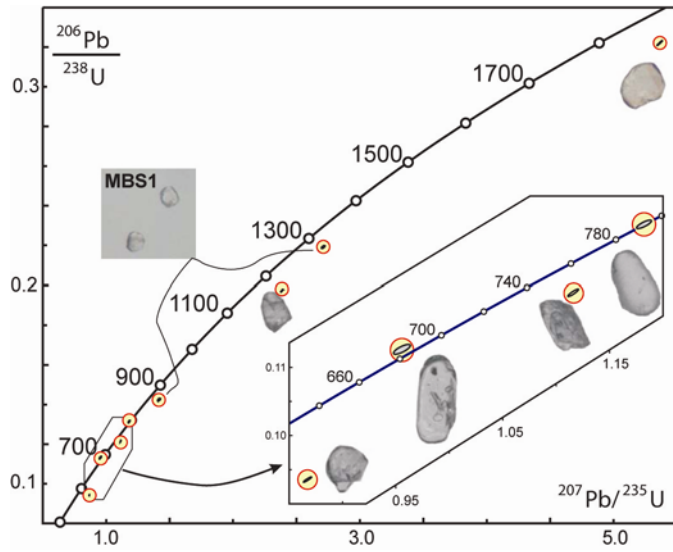


Figure 1 | Crustal thickness map based on gravity inversion and the Réunion hotspot chain.



**Figure 2 | U-Pb concordia diagram.**

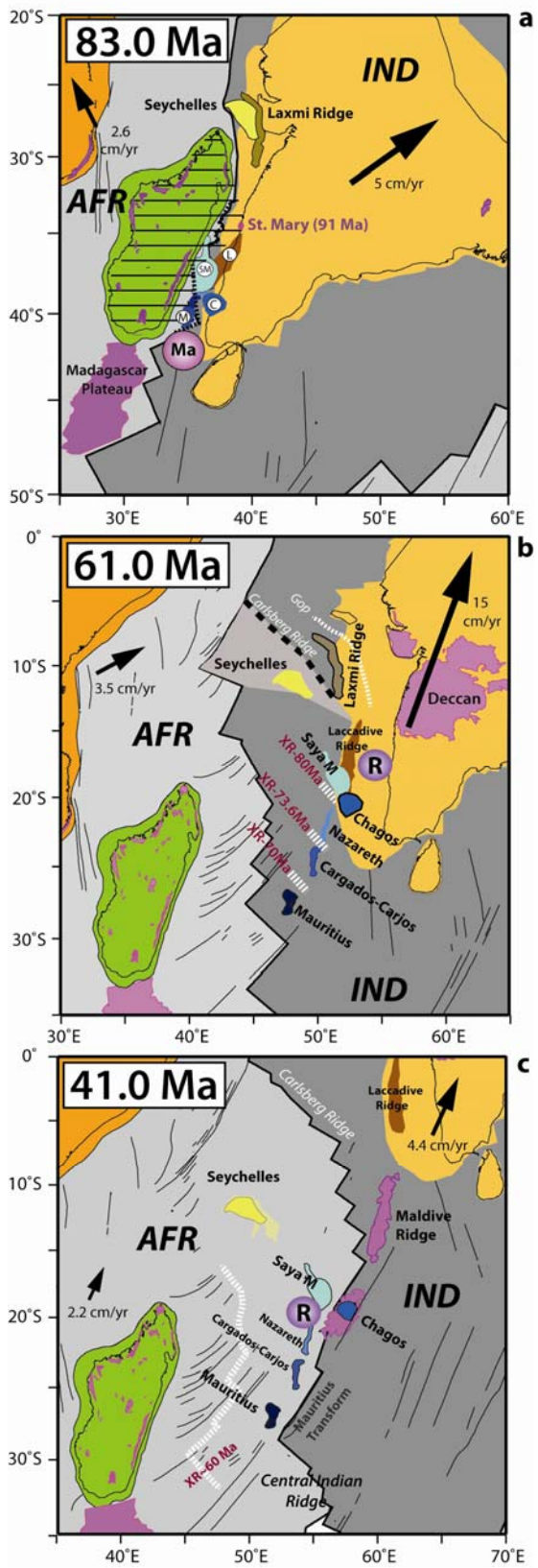


Figure 3 | Late Cretaceous to Eocene plate reconstructions.

# Supplementary Information

belonging to the article:

**A lost continent in the Indian Ocean**

## Plate reconstructions

Late Cretaceous and Tertiary plate configurations were reconstructed in a new global moving hotspot (mantle) reference frame<sup>1</sup>, based on radiometric age data from the best-studied hotspot tracks (Hawaiian, Louisville, New England, Tristan and Réunion) and numerical estimates of hotspot motion. For the past 50 Myr, this reference frame show gross similarities with the global mantle frames of Steinberger et al.<sup>2</sup> and Torsvik et al.<sup>3</sup>, but differ by some 5-10° in longitude for Africa at 70 and 80 Ma. Relative plate motions are listed in Torsvik et al.<sup>3</sup>, but important modifications with relevance to this study include the estimates of Neogene extension within the African plate due to the opening of the East African Rift system, and updated Cenozoic reconstructions of the Indian Ocean basin<sup>4</sup>.

The reconstructions presented in this paper describe one possible scenario of microcontinent dispersal between India and Madagascar from Mid Cretaceous to Oligocene. This model builds upon published reconstructions of the Seychelles microcontinent, the Laxmi Ridge and the Laccadives Ridges for the Mid-Cretaceous to Early Cenozoic<sup>5-6</sup>, but suggests that additional continental fragments (part of Saya del Maha, Nazareth Bank, Cargados-Carjos and Mauritius) were detached from the passive margins while seafloor spreading initiated in the Mascarene Basin. This scenario is presented in a novel set of reconstructions for the Mauritia inferred continental fragments (Fig. 3 and S5) where they were gradually transferred from the African plate to the Indian plate by a series of ridge jumps from Mid-Cretaceous to Early Cenozoic, and back to the African plate when a major plate reorganisation led to the establishment of the Central Indian Ridge in the Mid to Late Paleocene. The ages of these ridge jumps (extinct ridges) are mainly inferred from the geometry of plate boundary at the relevant times and considering that the south westernmost spreading corridor of the Mascarene basin seems to be highly asymmetric, with more crust on the NE flank (Fig. S4A). Interpretation of magnetic anomalies on the SW flank of south Mascarene Basin suggests a ~59 to ~70 Ma oceanic crust (Fig. S4). Although older magnetic anomalies (chrons 32 and 33, ~71-79 Ma) have been presented by previous studies (e.g.<sup>7</sup>) we argue that they cannot be confidently identified, especially in the north-eastern flank where subsequent hotspot volcanism obscures the original magnetic signature. Based on our new plate model we have produced a new seafloor age grid for the Indian Ocean (Fig. S7).

The 750 Myr reconstruction (Fig. S3) marks the birth of the Seychelles and is based on palaeomagnetic data from India<sup>9-10</sup> and the Seychelles<sup>11</sup>. The reconstruction is similar to that of Torsvik et al.<sup>11</sup> but here includes the Laxmi Ridge and Mauritia continental fragments between Southern India and Madagascar.



## Gravity inversion

Gravity inversion to determine Moho depth, crustal thickness and continental lithosphere thinning variation for the NW Indian Ocean was carried out in the 3D spectral domain using a method based on Parker<sup>12</sup> and incorporates a lithosphere thermal gravity anomaly correction (Fig. S1b) for both oceanic and continental margin lithosphere. The details of the methodology are described in Greenhalgh & Kuszniir<sup>13</sup> and Chappell & Kuszniir<sup>14</sup>. Data used in the gravity inversion are free-air gravity anomaly<sup>15</sup>, bathymetry<sup>16</sup> and sediment thickness<sup>17</sup>. A correction is made for crustal volcanic addition due to decompression melting during breakup and sea-floor spreading and uses a parameterization of the decompression melting model of White & McKenzie<sup>18</sup>. The gravity anomaly contribution from sediments assumes a compaction-controlled sediment density increase with depth. Thinned continental lithosphere and oceanic lithosphere has an elevated geothermal gradient; failure to incorporate a lithosphere thermal gravity anomaly correction gives a substantial over-estimate of crustal thickness predicted by gravity inversion. The lithosphere thermal gravity anomaly correction is calculated using a 3D lithosphere thermal model incorporating the spatial distribution of lithosphere geotherm perturbation and thermal re-equilibration time. Lithosphere thermal perturbation is defined using lithosphere thinning factor  $(1-1/\beta)$  and the model of McKenzie<sup>19</sup>. For continental margin lithosphere, the thermal re-equilibration (cooling) time is the breakup age of the continental margin and the lithosphere thinning factors used to define the lithosphere thermal perturbation are derived from the gravity inversion. For oceanic lithosphere, the thermal re-equilibration time corresponds to its age, which is obtained from oceanic isochrons, initially using Müller et al.<sup>20</sup> and subsequently refined with our own age grid (Fig. S7). An ocean lithosphere thinning factor of 1 is used to define the initial oceanic lithosphere thermal perturbation (Fig. S1c). Errors in the location and age of the oldest oceanic isochrons adjacent to a rifted continental margin would cause errors in lithosphere thermal gravity anomaly correction and therefore errors in crustal thickness determined from gravity inversion. Consequently the oldest ocean isochrons are not used to define oceanic lithosphere in the lithosphere thermal model; the resulting continental lithosphere thinning map produced by the gravity inversion gives an isochron-independent estimate of ocean-continent transition location. For the focus area of this study, the lithosphere thermal model used to determine the thermal gravity anomaly correction uses a continental breakup age of 65 Ma. The reference crustal thickness used in the gravity inversion is 36 km determined by calibration against seismically determined oceanic Moho depths west of India. Superposition of illuminated satellite gravity data onto crustal thickness maps from gravity inversion shows tectonic features (transform

faults and ocean ridges), rift orientation, continental breakup trajectory and possible pre-separation conjugacy (e.g. Chagos and Mascarenes in Fig. 1).

As discussed in Chappell & Kusznir<sup>14</sup>, the gravity inversion for Moho depth<sup>12</sup> is carried out in the wave-number domain, and in order to satisfy Smith's<sup>21</sup> theorem we must use constant crust and mantle densities. For the mantle we use  $3300 \text{ kg/m}^3$ , which we also use for calculating the lithosphere thermal gravity anomaly<sup>19</sup>, and is within the restricted range of densities suggested by the composition of mantle rocks<sup>22</sup>. Studies show that the mean densities of both continental and oceanic crust are close to  $2850 \text{ kg/m}^3$  (e.g.<sup>23,24</sup>). By adopting this assumption of constant crustal density of  $2850 \text{ kg/m}^3$  in the gravity inversion, our Moho depth prediction will tend to be shallower in regions of relatively dense crustal basement and deeper in regions of relatively light crustal basement. The sensitivity of predicted crustal thickness from gravity inversion to crustal basement density variation between  $2800$  and  $2900 \text{ kg/m}^3$  (an over-estimate of the likely range) is shown in Figure S2 and does not significantly change the distribution of thin and thick crust determined from gravity inversion. The use of identical densities for oceanic and continental crust and mantle also means that we do not prejudice the gravity inversions results with errors in a priori information of the distribution of oceanic and continental lithosphere (e.g. by using ocean isochrons). As a consequence the lithosphere thinning factor predicted by gravity inversion may be used to give an independent prediction of continent-ocean boundary location.

## Supplementary Table S1 | U-Pb isotopic data from zircons recovered from Mauritius sand

Characteristics <sup>1</sup>	Weight	U	Th/U <sup>2</sup>	Pbc <sup>3</sup>	<sup>206</sup> Pb/ <sup>204</sup> Pb <sup>4</sup>	<sup>207</sup> Pb/ <sup>235</sup> U <sup>5</sup>	± 2σ	<sup>206</sup> Pb/ <sup>238</sup> U <sup>5</sup>	± 2σ	rho	<sup>207</sup> Pb/ <sup>206</sup> Pb <sup>5</sup>	± 2σ	<sup>206</sup> Pb/ <sup>238</sup> U <sup>5</sup>	<sup>207</sup> Pb/ <sup>235</sup> U <sup>5</sup>	<sup>207</sup> Pb/ <sup>206</sup> Pb <sup>5</sup>
	[μg]	[ppm]		[pg]			[abs]		[abs]			[abs]	[age in Ma]		
<b>E04-1; S20°03'10"</b>															
<b>E57°31'19"</b>															
eq sb c	10	165	0.49	3.5	9627	5.365	0.018	0.32156	0.00106	0.97	0.12100	0.00010	1797	1879	1971
tip an-sb	1	1123	0.33	4.1	3384	2.385	0.009	0.19671	0.00066	0.93	0.08795	0.00011	1158	1238	1381
eq an p	6	1108	0.12	6.5	6008	0.868	0.003	0.09357	0.00031	0.93	0.06724	0.00008	577	634	845
el an y cr	9	310	0.28	4.6	4659	1.115	0.004	0.12092	0.00044	0.91	0.06691	0.00010	736	761	835
el an fr c	14	73	0.94	5.1	1667	1.182	0.006	0.13088	0.00051	0.81	0.06548	0.00018	793	792	790
el sb c in	16	72	0.52	12.8	651	0.956	0.006	0.11265	0.00059	0.77	0.06153	0.00027	688	681	658
<b>MBS1; S20°22'16"</b>															
<b>E57°42'04"</b>															
eq an c	<1	>170	0.20	2.1	1127	2.711	0.013	0.21849	0.00066	0.63	0.09000	0.00033	1274	1332	1425
eq an c	<1	>220	0.17	2.8	695	1.417	0.010	0.14188	0.00056	0.61	0.07245	0.00041	855	896	999

<sup>1</sup>) All analyses of single zircon grains, not abraded; sb = subhedral; an = anhedral; eq = equant; el = elongated; p = pink; y = yellowish; c = clear; cr = cracks; fr = frosted surface; in = inclusions.

<sup>2</sup>) Th/U model ratio inferred from 208/206 ratio and age of sample. <sup>3</sup>) total amount of common Pb (initial + blank). <sup>4</sup>) raw data corrected for fractionation. <sup>5</sup>) corrected for fractionation, spike, blank and initial common Pb; error calculated by propagating the main sources of uncertainty.

The zircons were analysed for U and Pb isotopes by ID-TIMS (University of Oslo). Decay constant are from Jaffey et al.<sup>45</sup>. The data were corrected for blanks of 2 pg for Pb and 0.1 pg for U. Details of the analytical procedure are given in Corfu<sup>46</sup>.

## Supplementary Table S2 | Absolute and relative plate reconstruction parameters

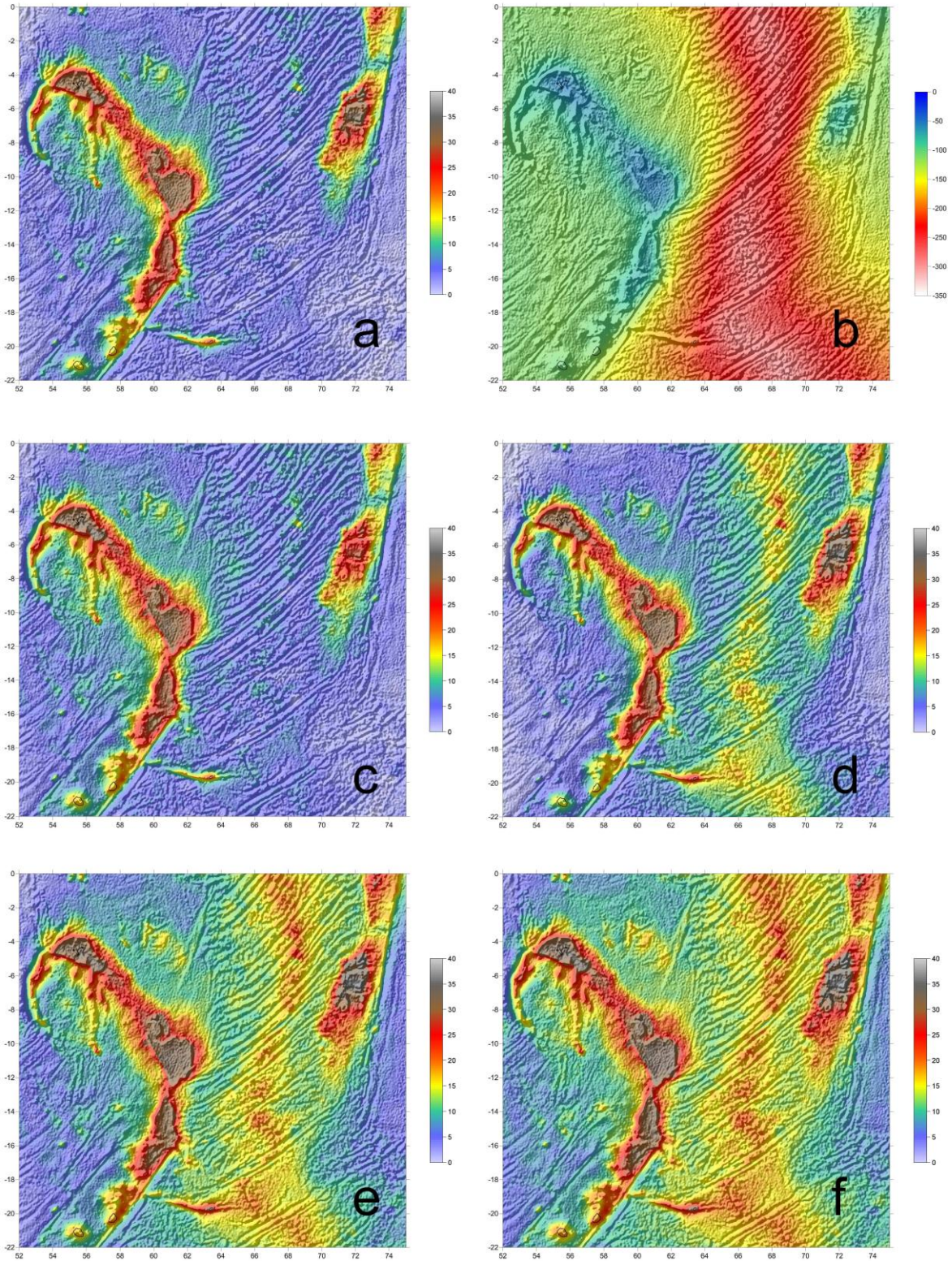
(a) Absolute plate reconstruction of South Africa (SAF) and Madagascar (MAD). These are approximately the same for the past 120 Myr because MAD was part of the Somalian plate since then and we use a plate model with very small adjustments of Somalia vs. SAF.

Age (Ma)	Plate	Euler rotation		
		Lat	Lon	Angle
16	SAF, MAD	37.7	-27.1	-2.8
33	SAF, MAD	36.7	-27.6	-6.9
41	SAF, MAD	38.1	-31.5	-9.2
56	SAF, MAD	48.2	-31.5	-10.6
61	SAF, MAD	51.1	-30.9	-11.7
73.6	SAF, MAD	43.4	-28.4	-16.8
83.5	SAF, MAD	27.8	-24.5	-20.0

(b) Relative fits vs. a fixed Madagascar for India, Seychelles, Laxmi Ridge and the Mauritian elements (numbers in brackets are plate ID numbers used in GPlates, [www.gplates.org](http://www.gplates.org)).

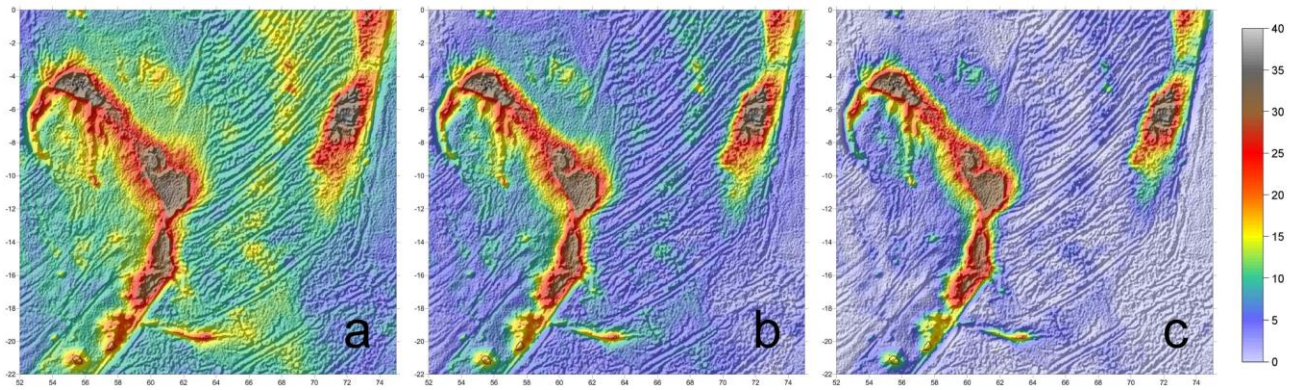
Age (Ma)	India (501)			Seychelles (704)			Saya de Malha (705)			Laxmi Ridge (570)		
	Lat	Lon	Angle	Lat	Lon	Angle	Lat	Lon	Angle	Lat	Lon	Angle
16	24.8	29.3	-6.4	0.0	0.0	0.0	0.0	0.0	0.0	24.8	29.3	-6.4
33	20.6	42.4	-16.0	0.0	0.0	0.0	0.0	0.0	0.0	20.6	42.4	-16.0
41	20.6	44.3	-19.9	0.0	0.0	0.0	0.0	0.0	0.0	20.6	44.3	-19.9
56	18.2	32.3	-31.9	0.0	0.0	0.00	0.0	0.0	0.0	18.2	32.3	-31.9
61	15.5	31.0	-38.5	-22.9	60.8	-5.8	-0.3	35.6	-3.3	15.5	31.0	-38.5
73.6	19.5	21.9	-48.1	-5.7	46.6	-31.3	-0.3	35.6	-24.1	16.4	24.6	-45.8
83.5	23.5	19.7	-51.5	2.4	42.7	-32.7	9.9	32.08	-26.1	20.8	22.2	-48.9

Age (Ma)	Laccadive Ridge (572)			Chagos (573)			Cargados-Barjos Bank (575)			Mauritius (577)		
	Lat	Lon	Angle	Lat	Lon	Angle	Lat	Lon	Angle	Lat	Lon	Angle
16	24.8	29.3	-6.4	13.7	47.4	-9.6	0.0	0.0	0.0	0.0	0.0	0.0
33	20.6	42.4	-16.0	13.3	49.8	-19.7	0.0	0.0	0.0	0.0	0.0	0.0
41	20.6	44.3	-19.9	19.8	48.5	-19.0	0.0	0.0	0.0	0.0	0.0	0.0
56	18.2	32.3	-31.9	19.8	48.5	-19.0	0.0	0.0	0.0	0.0	0.0	0.0
61	15.5	31.0	-38.5	16.6	47.0	-22.1	-0.3	35.6	-3.3	-0.3	35.6	-3.3
73.6	11.8	32.5	-56.4	7.4	43.0	-42.2	-0.3	35.6	-24.1	-4.8	39.1	-22.9
83.5	15.5	29.9	-59.1	12.6	39.8	-44.6	6.2	36.0	-24.6	-0.6	43.6	-22.5

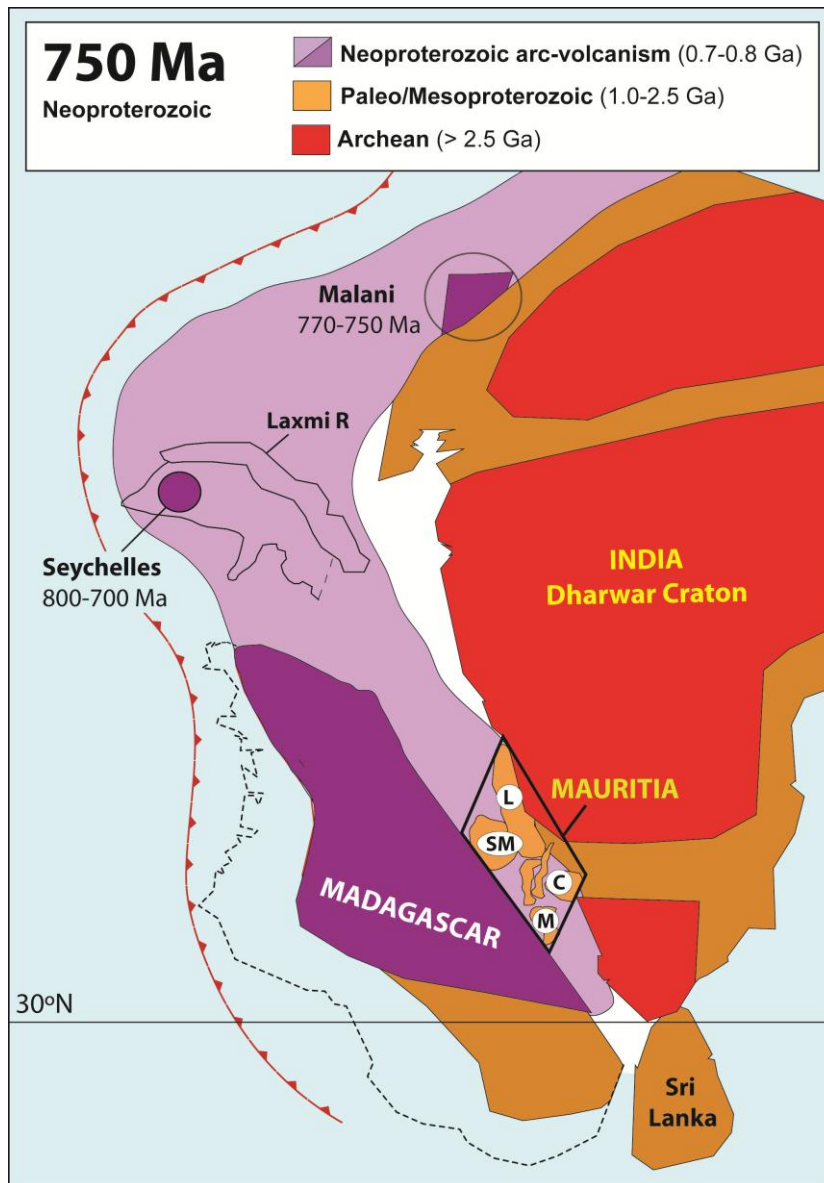


**Supplementary Fig. S1 | Gravity inversion sensitivity test.** Sensitivity of crustal thickness (in km) determination from gravity inversion to age of lithosphere thermal perturbation used in the gravity inversion to determine the lithosphere thermal gravity anomaly correction. Changing the oceanic lithosphere thermal model has a major effect on oceanic crustal thickness determined by

gravity inversion but not crustal thickness under the Seychelles, Mascarenes or Chagos. **a**, Crustal thicknesses estimated using ocean isochrons (Fig. S7) to determine lithosphere thermal cooling time only but with the lithosphere thinning factor used to determine the magnitude of the lithosphere thermal perturbation determined from gravity inversion for both oceanic and continental regions. Lithosphere thermal re-equilibration time for regions with no oceanic isochrons is 65 Myr. **b**, Corresponding lithosphere thermal gravity anomaly correction. **c**, As in (a) but using ocean isochrons to give lithosphere thinning factor = 1 for oceanic regions for determining lithosphere thermal gravity anomaly correction. **d**, No ocean isochrons used. Lithosphere thermal cooling time of 40 Myr. **e**, As in (d) but with lithosphere thermal cooling time of 65 Myr. **f**, As in (d) but with lithosphere thermal cooling time of 85 Myr.

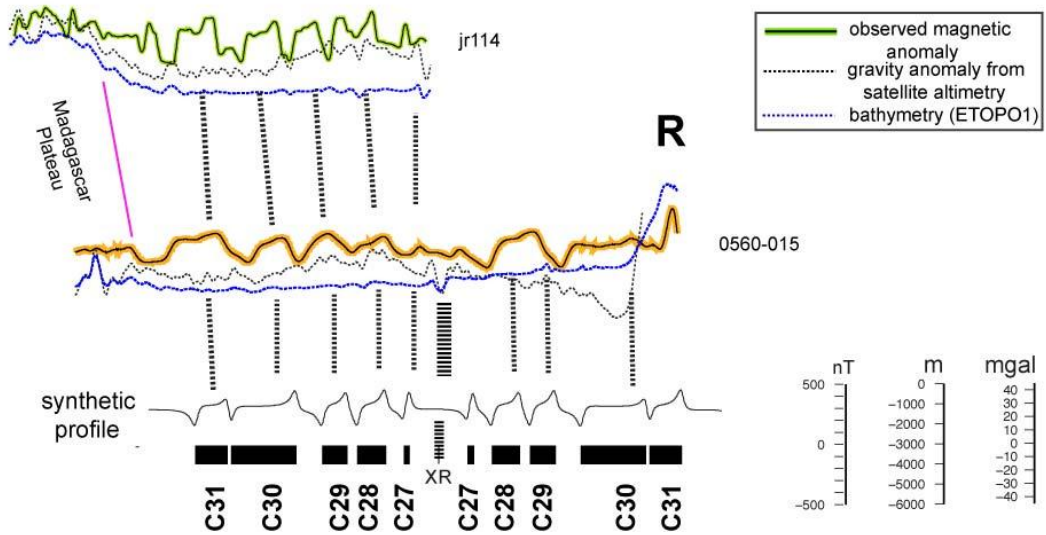
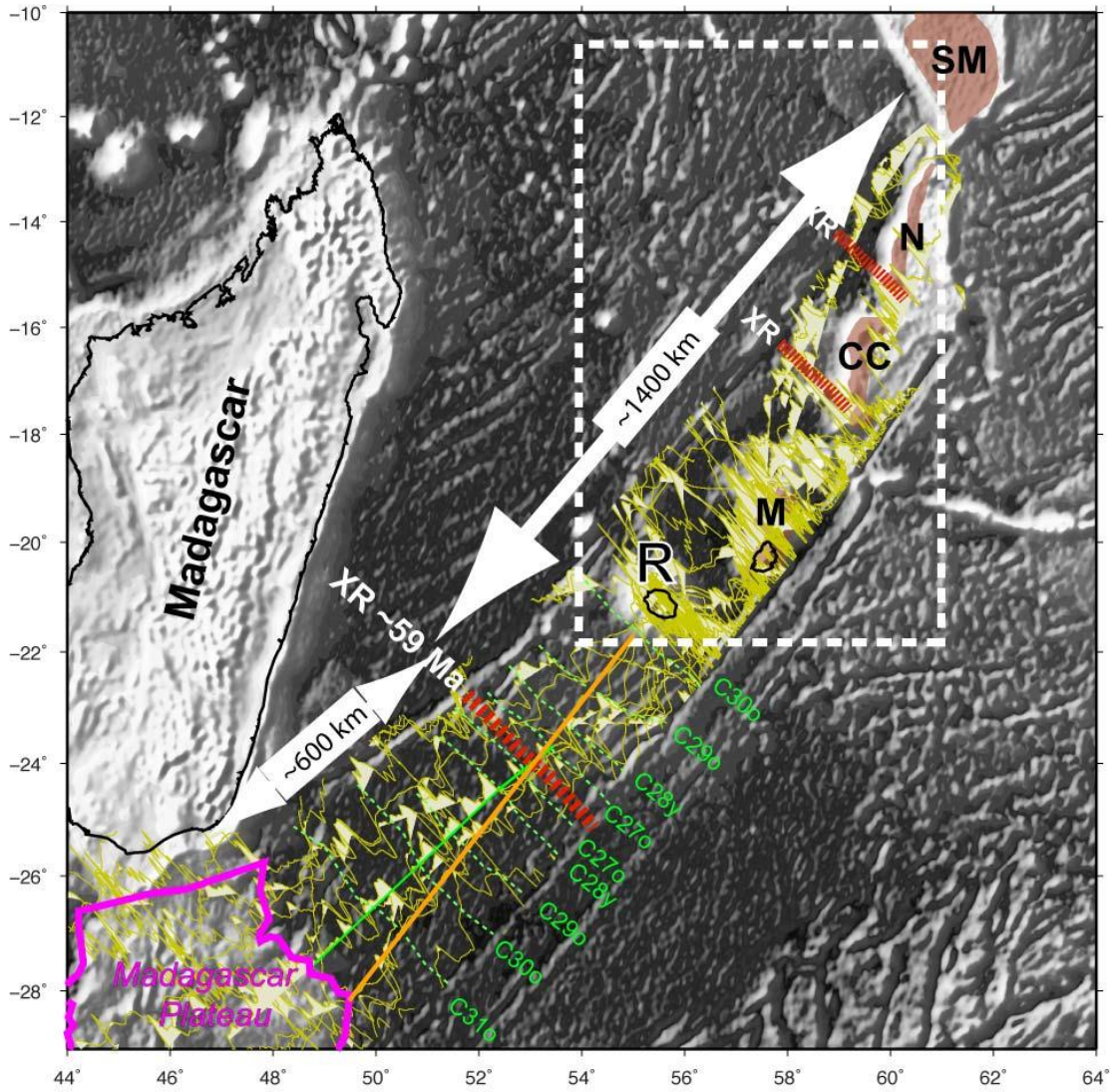


**Supplementary Fig. S2 | Crustal basement density sensitivity test.** Sensitivity of crustal basement thickness (in km) predicted by gravity inversion to crustal basement density. **a**, density = 2800 kg/m<sup>3</sup>. **b**, density = 2850 kg/m<sup>3</sup>. **c**, density = 2900 kg/m<sup>3</sup>. Other inversion parameters are the same as used in Figure 1. The preferred value of crustal basement density is 2850 kg/m<sup>3</sup>. The sensitivity test (and in Fig. S1) is shown for the Mascarene Plateau region (Seychelles to Mauritius) and the conjugate Chagos Bank that was joined to the Southern Mascarene Plateau (Saya de Malha and Nazareth Banks) before 41 Ma.



**Supplementary Fig. S3 | Neoproterozoic plate reconstruction.** 750 Ma reconstruction of India-Madagascar-Seychelles, Mauritius (M) and other potential Proterozoic continental fragments (e.g., SM, Saya de Malha; L, Laccadives; C, Chagos) that constitute Mauritia. The Laxmi Ridge, which now includes highly extended continental crust<sup>25</sup>, is considered Neoproterozoic in age and is juxtaposed with the Seychelles. These Neoproterozoic arc fragments, along with Mauritia and India, broke away from Madagascar after 83.5 Ma. India and Madagascar were joined during and possibly before the formation of the Rodinia supercontinent at ~1100 Ma, and Mauritia contains Palaeoproterozoic continental crust that underwent Neoproterozoic reworking/magmatism, similar to that of India and Madagascar. Known areas of Neoproterozoic arc-magmatic activity are shown in dark magenta whereas areas of postulated activity of that age are shown in light magenta. In our reconstruction, Madagascar and India were located at latitudes between 30 and 50°N at 750 Ma with Mauritia located between southern India and Madagascar.

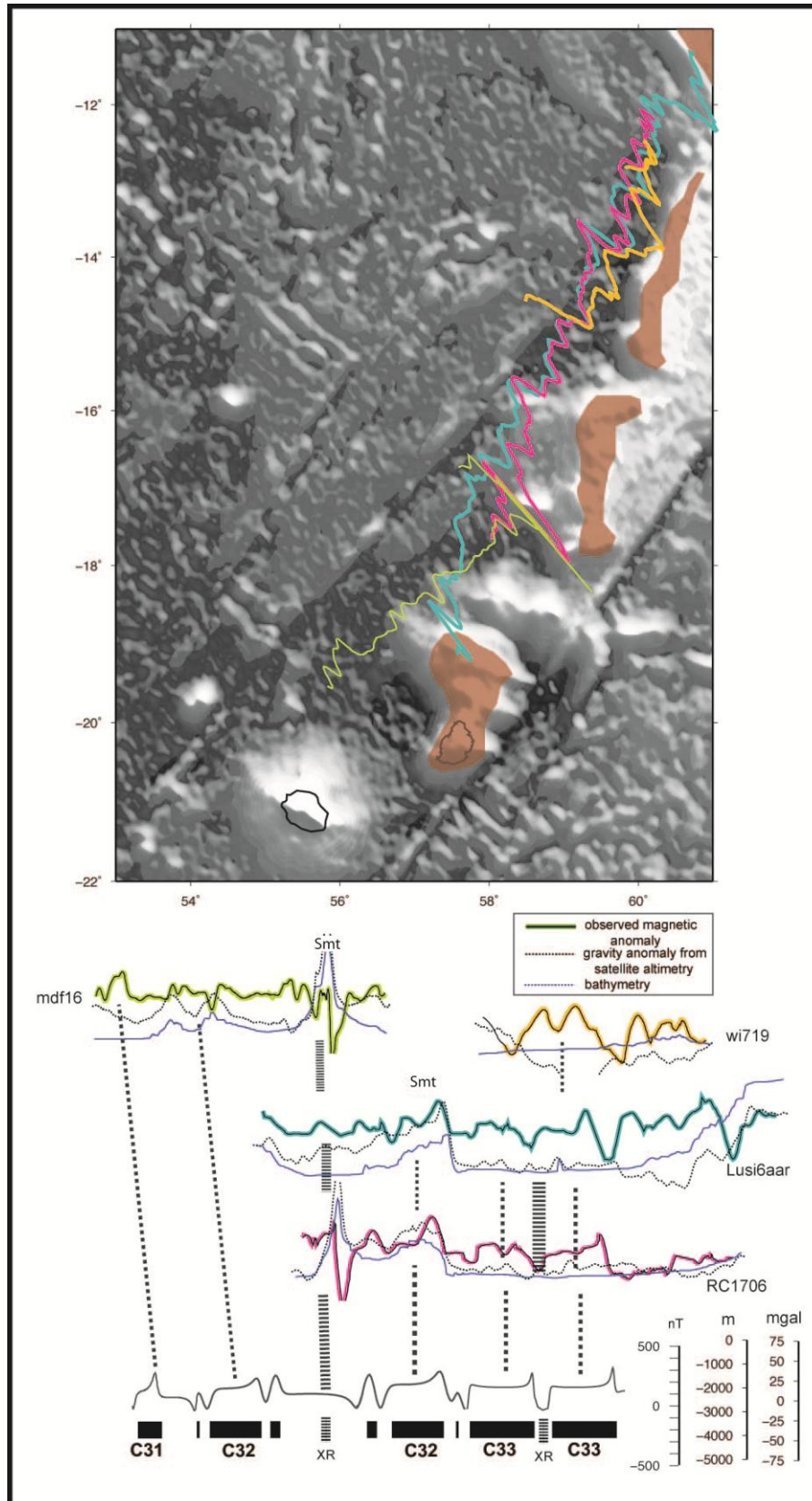




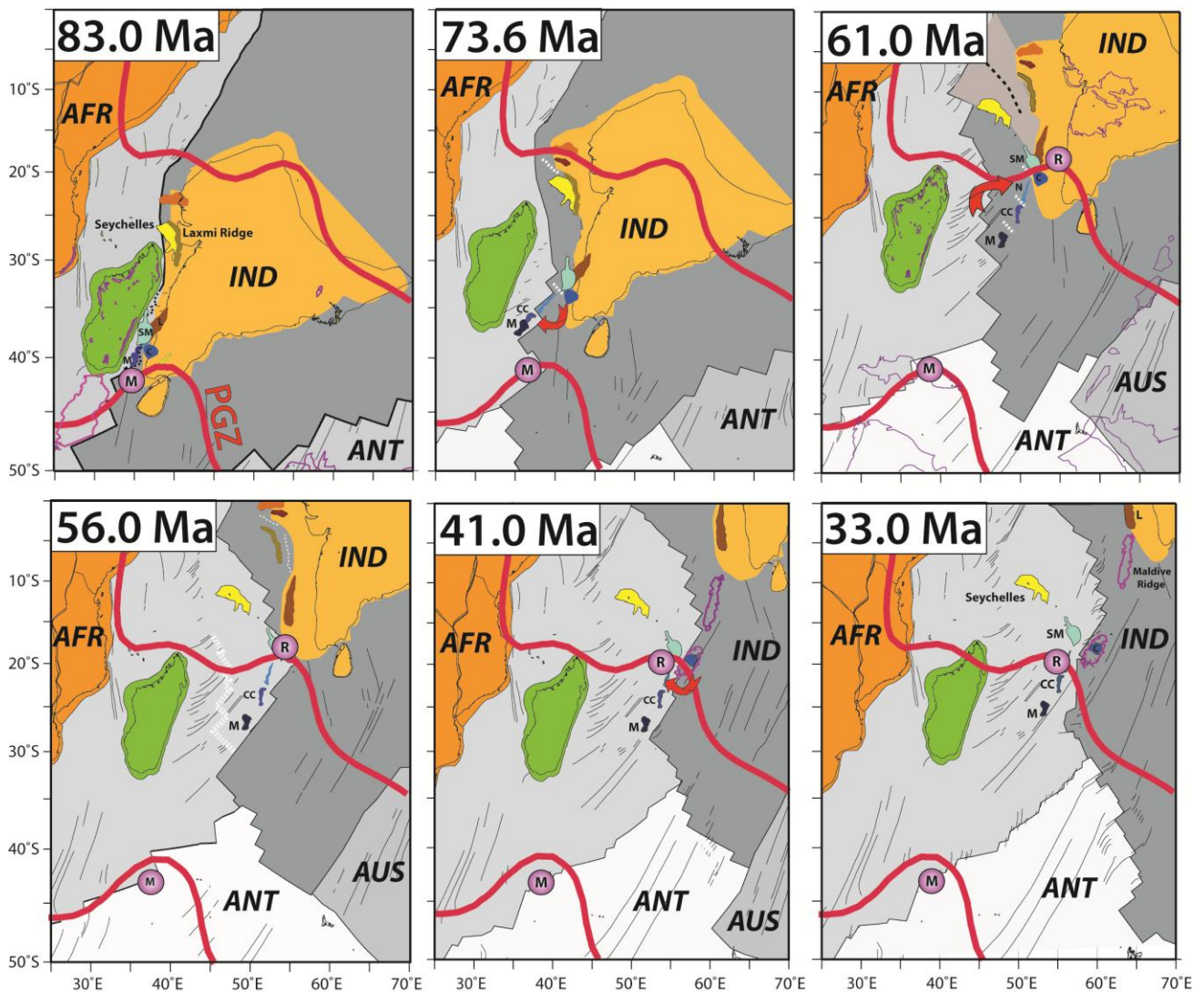
**Supplementary Fig. S4a | Magnetic anomalies in the south Mascarene basin.** Background image shows the illuminated (300° from north) residual gravity anomalies (free air gravity anomalies after

removal of regional anomalies) to illustrate the direction of major fracture zone and general fabric of oceanic crust. Note that the conjugate spreading corridors that flank the extinct late Paleocene mid ocean ridge (XR) are highly asymmetric with the SW part less than half than the NE one. This indicates that plate boundaries relocation accreted more oceanic crust on the NE flank through ridge jumps. Magnetic anomalies from selected ship track data are shown in the region between Mahanoro-Wilshaw (to the north) and Mauritius (to the south) fracture. Interpretation of chrons 27 to 31 on both flanks of the extinct ridge are shown as isochrons (dashed green lines). We also selected two magnetic profiles acquired from Mauritius to Madagascar Plateau (0560-015 from 1993) and from east of the extinct ridge to Madagascar Plateau (jr115 from 1987) and a synthetic profile to show our interpretation of magnetic anomalies. Oceanic crust between the youngest extinct ridge and the Reunion island is ~60 Ma (C30) and younger, as also suggested by Bernard & Munsch<sup>7</sup>. The difference between their interpretation and present study is the absence of the extinct ridge at C28 identified on the SW flank. We agree that such an interpretation could be made, and this will decrease even further the asymmetry between the two conjugate spreading corridors emphasizing the need for additional older than C30 extinct spreading ridges between Reunion and Saya del Malha. In order to identify such features, we interpret several magnetic profiles available for the region the Mascarene Plateau and Mauritius region (inset map and interpretation shown in Figure S4b). We have selected the cruises that cover the northernmost region presumably less affected by subsequent hotspot volcanism, however magnetic anomalies over seamounts show a larger amplitude and their overall shape may have been distorted by it. The data was collected between 1962 and 1978 (LUSI6AAR 1962, RC1706 1974, wi719, mdf16 1978).

The synthetic magnetic profiles used the following parameters: full seafloor spreading rates 65 km/Myr between 59 and 63 Ma, 100 Km/Myr between 63 and 72 Ma, and 50 km/Myr between 72 and 79 Ma; present day magnetic inclination  $-54^{\circ}$ , magnetic declination  $-18^{\circ}$ ; depth to magnetised body 4.5 km; strike of magnetised body  $120^{\circ}$ . R, Reunion; M, Mauritius; CC, Cargados-Carjos; N, Nazareth; SM, Saya de Malha.

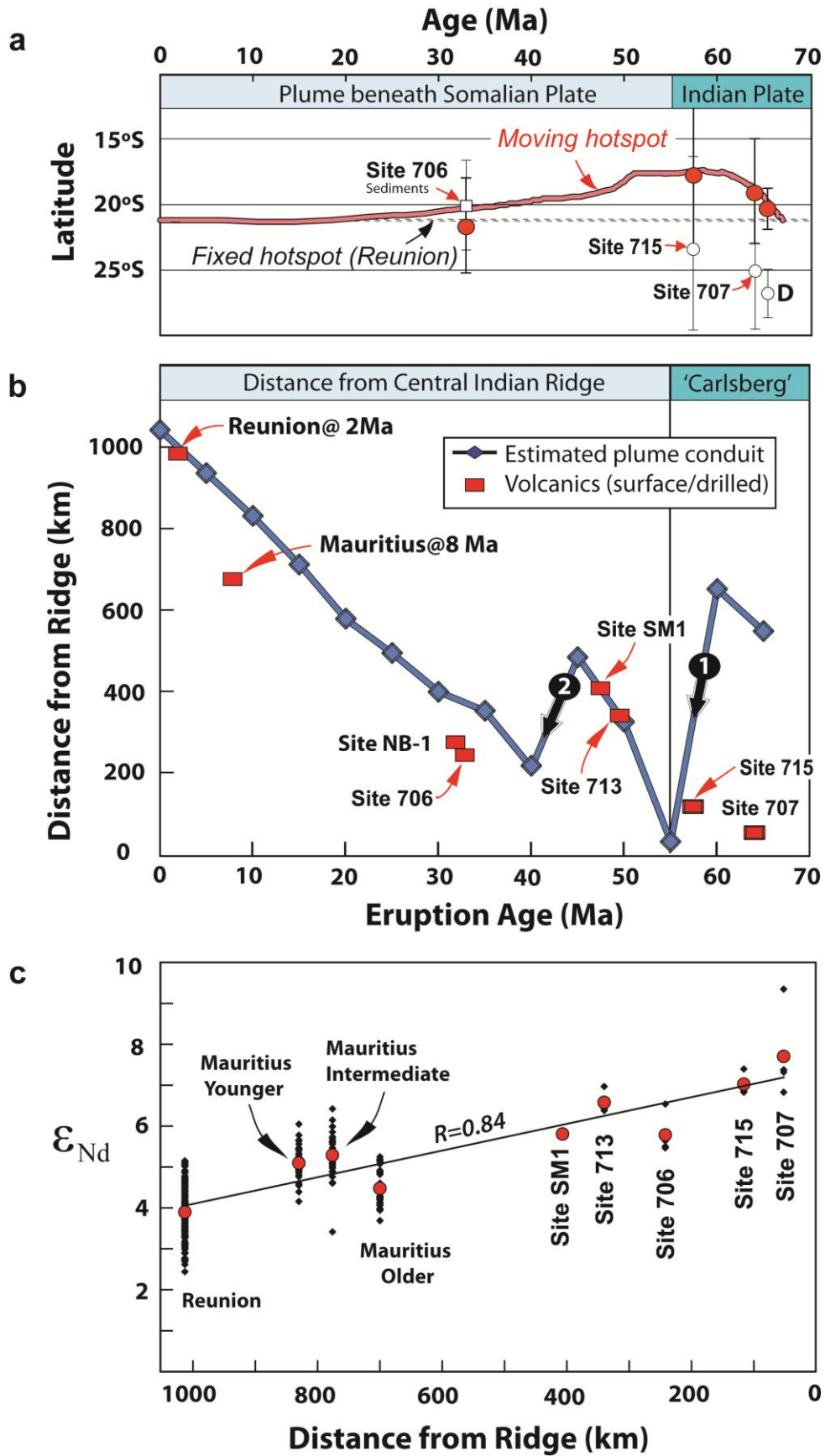


**Supplementary Fig. S4b | Detailed magnetic anomaly interpretation from Reunion to Saya de Malha.** The diagram represents the stippled area in Fig. S4a. Smt, seamount.



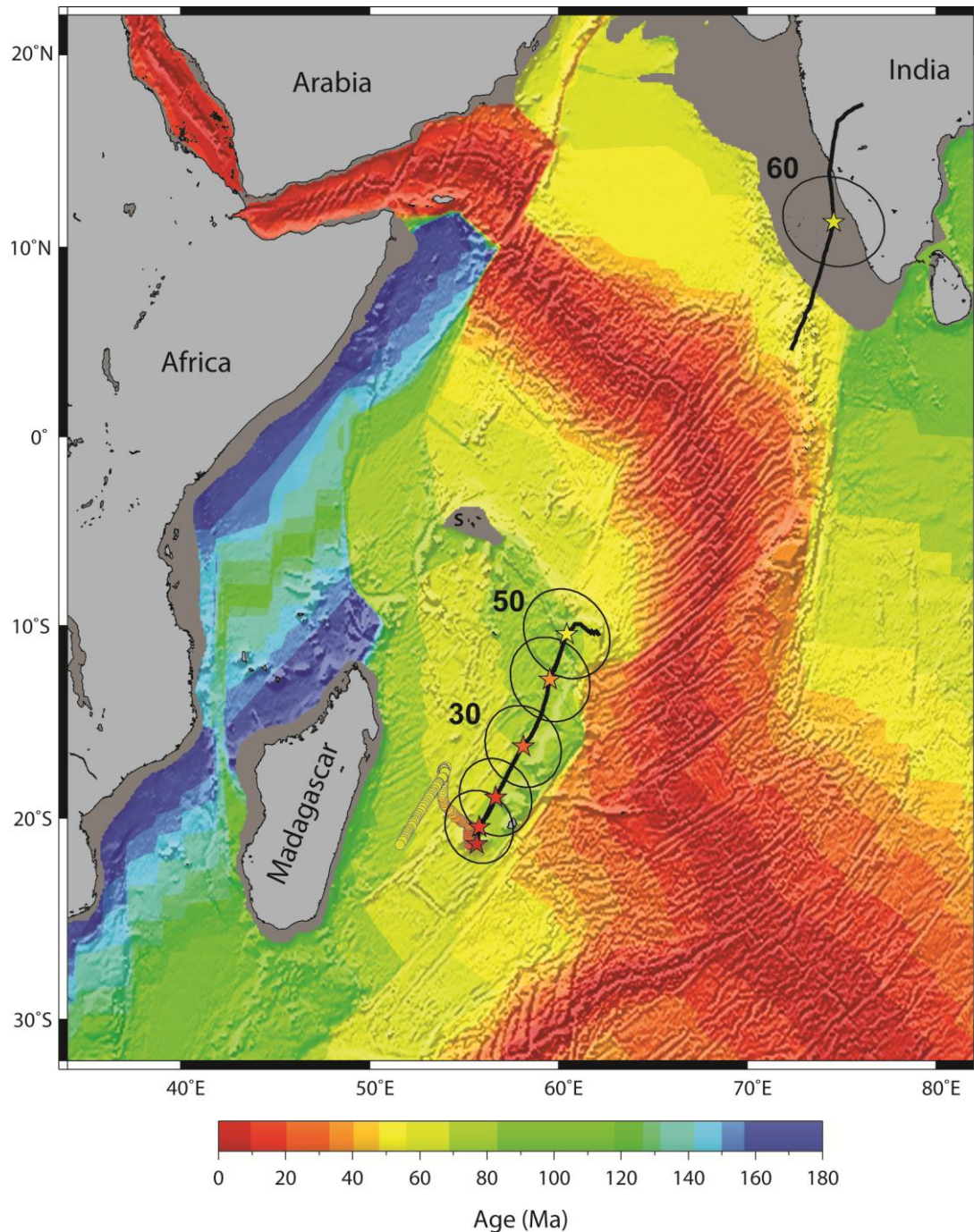
**Supplementary Fig. S5 | Plate tectonic reconstructions from the Late Cretaceous to Miocene in an absolute reference frame<sup>1</sup>.** The predicted positions of Marion (M) and Reunion (R) hotspots (corrected for plume advection; Fig. 1 *inset* diagram and Fig. S8) are shown in magenta, and the thick red lines are the plume generation zones (PGZs<sup>8</sup>) at the core-mantle boundary. Extinct spreading ridges between various microcontinents are shown as dashed white lines. We show that ridge jumps propagated SW while the Marion plume was in the proximity of the active plate boundary. Red arrows indicate direction of plate boundary relocation towards closest hotspot. Oceanic floor fabric and direction of spreading between major tectonic plates is depicted by interpreted fracture zones<sup>26</sup>. Major plate boundaries are shown as thick black lines. Outlines of major volcanic plateaus and provinces are shown in magenta. AFR, Africa; IND, India, AUS, Australia; ANT, Antarctica.

At ~83.0 Ma India, along with the Seychelles/Laxmi Ridge and some Mauritian continental fragments (SM, Saya de Malha; L, Laccadives; C, Chagos) separated from Madagascar, whilst Mauritius (M), Cargados-Carjos (CC) and the Nazareth (N) banks belonged to Madagascar. This occurred shortly after a major magmatic event linked to the Marion plume, which affected most of Madagascar, parts of India, and the offshore Madagascar Plateau. The plume centre was probably located near the southern tip of Madagascar. During opening of the Mascarene Basin (83.5 to 61 Ma) we model three major ridge jumps at 80, 73.6 and 70 Ma (thick dashed white extinct ridges in 61 Ma reconstruction). Mauritius and other potential parts of Mauritia were gradually transferred to the Indian plate, and after 70 Ma all of Mauritia was part of the Indian plate. Following peak Deccan magmatism at around 65.5 Ma, seafloor spreading was initiated between the Laxmi Ridge and the Seychelles (62-63 Ma) but seafloor spreading was still ongoing in the Mascarene Basin. After 61 Ma, there was a radical change in the Indian Ocean architecture: the Reunion plume was now located beneath the SW margin of India; this probably assisted a major NE ridge-jump that led to the termination of seafloor spreading in the Mascarene Basin shortly after chron 27. By 56 Ma, Mauritian fragments (except Laccadives) and the Seychelles became part of the African plate. Thereafter, the Reunion Plume was beneath the slowly moving African plate. An important ridge-jump occurred at ~41 Ma when the Réunion plume was located at the position of Saya de Malha/Nazareth. This ridge jump led to separation of Chagos from other Mauritian elements and Chagos once again became part of the Indian plate.



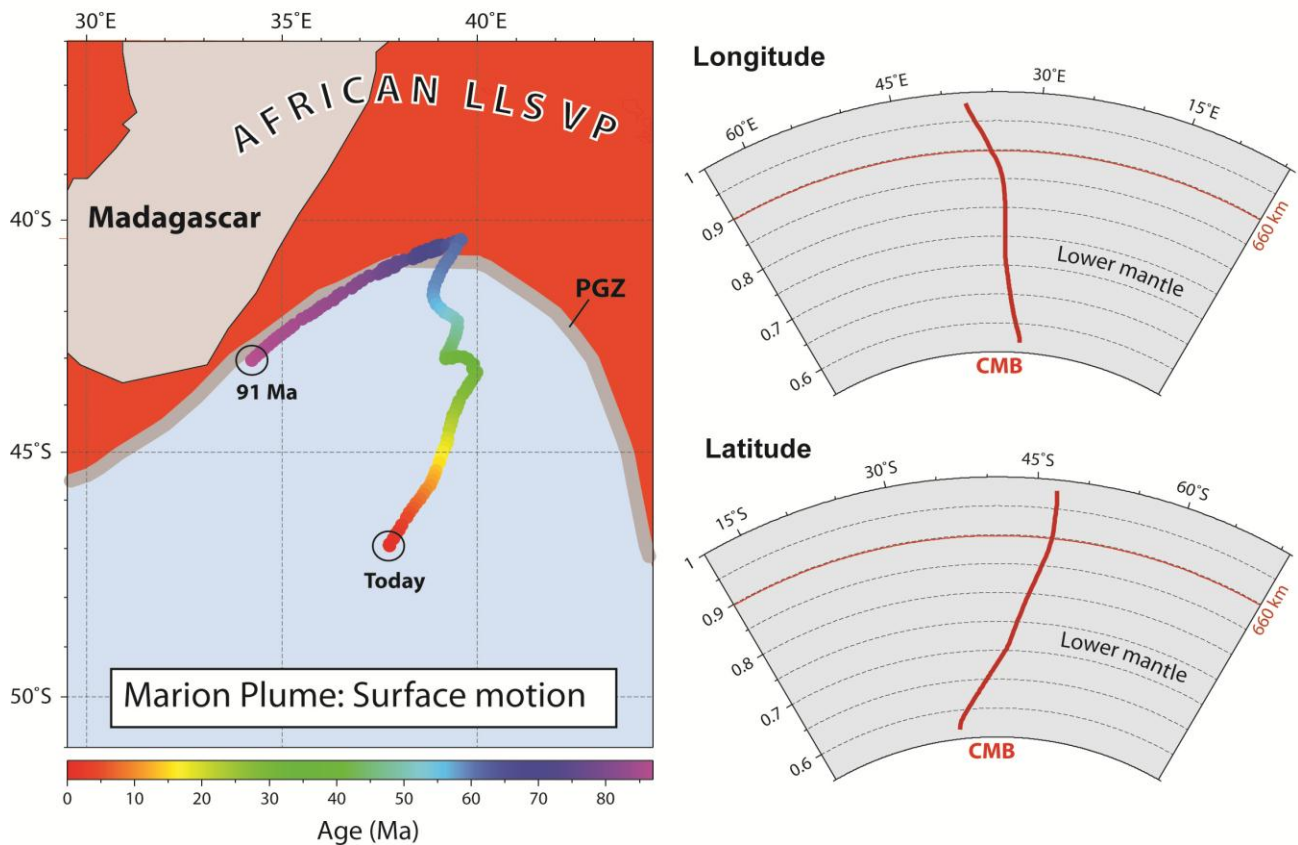
**Supplementary Fig. S6 | Palaeolatitudes, distance from ridge and  $\epsilon_{Nd}$ .** a, Palaeomagnetically-determined palaeolatitudes for the Réunion hotspot chain. The Réunion plume lay beneath the

Deccan LIP at ~65.5 Ma, and in our global plate model<sup>1</sup> the cross-over from the Indian to the Somalian plates occurred at ~55 Ma when the hotspot was beneath the Saya de Malha Bank (Fig. 1). Palaeomagnetic data from ODP Leg 115 Sites 706, 707 and 715 (open white circles/square) from Schneider & Kent<sup>27</sup> and Vandamme & Courtillot<sup>28</sup>. The palaeolatitude of the Deccan (D) traps is based on a mean of seven studies listed in Torsvik et al.<sup>3</sup> (Pole = 38.2°S, 101.2°E, A95=2.3°, Palaeolatitude = 26.8°S <sup>+1.9</sup>/<sub>-1.8</sub> recalculated to a reference site of 20°N and 75°E). Double stippled line assumes a fixed Réunion hotspot, whereas the thicker red line is the calculated plume conduit advection from our global mantle model<sup>1</sup>. Note that Site 706 is a sedimentary site and is likely affected by inclination-shallowing. The data are also shown after true polar wander correction (filled red circles): Palaeomagnetic data from Sites 715 and 707 have been long known<sup>28</sup> to predict higher latitudes than fixed or moving hotspot models, but correcting for true polar wander leads to an excellent fit with our moving hotspot model. True polar wander correction<sup>1</sup> changes the Deccan palaeolatitude from 26.8°S to 20.4°S, Site 707 from 25.2°S to 19.2°S, Site 715 from 23.6°S to 17.8°S and Site 706 from 20.2°S to 21.8°S. **b**, Distance between spreading ridge and the Réunion plume conduit and dated volcanic rocks. We computed the distance between the modelled plume conduit and the nearest spreading ridge (based on our new seafloor age grid) through time using a global moving hotspot model in which the data from the Reunion hotspot track were not used for the definition of absolute plate motion (Fig. S7). At 65 and 60 Ma, the distance to the nearest spreading ridge varied between 550 and 650 km. During this time period, volcanism at Site 707 (now part of the North Mascarene Plateau; Fig. 1) dated to 64.1 Ma, as well as assumed Deccan related magmatism on the Seychelles (63.5 Ma) occurred far away from the Réunion plume conduit but near the Gop Rift and Carlsberg ocean ridges (Fig. 3b). A dramatic relocation of spreading ridges after 61 Ma (Mascarene spreading stopped and the Central Indian Ridge linked up with the Carlsberg Ridge) was probably imposed by a vigorous plume. The Réunion plume was for a short while directly interacting with the ridge (at ~55 Ma), but soon after crossed the ridge and lay beneath the African plate thereafter. Eruptive activity at Site 715 on the Indian plate occurred near the spreading ridge at 57.5 Ma, shortly before plate cross-over and was thus located near the spreading ridge. The modelled plume-ridge distance increased between 55 and 45 Ma to nearly 500 km (Site 713 and Site SM1 erupted ca. 250-350 km from the ridge) but thereafter a second important ridge jump took place and Chagos separated from Mauritania on the African plate, and became part of the Indian plate. This led to a short period of plume-ridge interaction but the plume-ridge distance has increased systematically (not affected by ridge jumps) for the past 40 Myr. The distance between Mauritius and Réunion to a ridge is shown at 8 and 2 Ma. The black circles with numbers 1 and 2 denote the important Tertiary ridge-jumps. **c**,  $\epsilon_{Nd}$  in lavas from Réunion, Mauritius and ODP115 sites vs. distance from spreading ridge. The data are plotted versus distance and not age, as normally done (e.g.<sup>29-30</sup>). With increased distance there is a systematic change to less MORB-like ( $\epsilon_{Nd} \sim 10$ ) values. The regression line (R=0.84) is calculated from average values (red solid circles). Data sources<sup>29-43</sup>.  $\epsilon_{Nd}$  not available from Site NB-1 in (b).



**Supplementary Fig. S7 | New seafloor age grid for the Indian Ocean.** Model track of the Réunion hotspot predicted using a global moving hotspot frame similar to that of Doubrovine et al.<sup>1</sup>, but excluding the data from the Reunion chain itself, is superimposed on the seafloor age grid. The African and Indian segments of the track, shown by the thick black lines with stars corresponding to the locations calculated at 10 Myr intervals, are plotted on our new seafloor age-grid. To highlight tectonic features, the age-grid was illuminated by the gradient derived from the ETOPO1 global topography and bathymetric model<sup>16</sup>. Circles, colour-coded according to the age, show the surface hotspot motion calculated at 1 Myr increments. S, Seychelles.





**Supplementary Fig. S8 | Modelled location of the Marion hotspot and present day plume conduit.** The left-hand panel shows the modelled surface location of the Marion hotspot with time, and is based on the absolute kinematic model of Doubrovine et al.<sup>1</sup> based on five hotspot track, including the Reunion chain. Surface trace of Marion hotspot is shown as rainbow-colored swath, color-coded according to the age. The surface location at 91 Ma (initiation time in this model) places the top of the plume near southern Madagascar, and close to the deep mantle plume generation zone (PGZ, thick grey line) at the core-mantle boundary (1% slow contour in the SMEAN tomographic model<sup>44</sup>). With time, the plume becomes advected in the mantle flow, and the right-hand panels show longitudinal and latitudinal cross-sections of the modelled Marion plume today.

## Supplementary References

1. Doubrovine, P.V., Steinberger, B. & Torsvik, T.H. Absolute plate motions in a reference frame defined by moving hotspots in the Pacific, Atlantic and Indian oceans. *J. Geophys. Res.* **117**, B09101 (2012).
2. Steinberger, B., Sutherland, R., & O'Connell, R.J. Prediction of Emperor-Hawaii seamount locations from a revised model of global plate motion and mantle flow. *Nature* **430**, 167-173.
3. Torsvik, T.H., Müller, R.D., Van der Voo, R., Steinberger, B. & Gaina, C. Global Plate Motion Frames: Toward a unified model. *Rev. Geophysics* **46**, RG3004 (2008).
4. Cande, S.C., Patriat, P. & Dymant, J. Motion between the Indian, Antarctic and African plates in the early Cenozoic. *Geophys. J. Int.* **183**, 127-149 (2010).
5. Calvès, G. *et al.* A. Seismic volcanostratigraphy of the western Indian rifted margin: The pre-Deccan igneous province, *J. Geophys. Res.* **116**, B01101 (2011).
6. Ganerød, M. *et al.* In *The Formation and Evolution of Africa: A Synopsis of 3.8 Ga of Earth History* (Eds Van Hinsbergen, D.J.J., Buiter, S.J.H., Torsvik, T.H., Gaina, C. & Webb, S.J.) Geological Society London Special Publications **357**, 229-252 (2011).
7. Bernard, A. & Munsch, M. Were the Mascarene and Laxmi Basins (western Indian Ocean) formed at the same spreading centre? *C. R. Acad. Sci. Paris, Sciences de la Terre et des planètes. Earth Planet. Sci.* **330**, 777-783 (2000).
8. Burke, K., Steinberger, B., Torsvik, T.H. & Smethurst, M.A. Plume Generation Zones at the margins of Large Low Shear Velocity Provinces on the core–mantle boundary. *Earth Planet. Sci. Lett.* **265**, 49-60 (2008).
9. Torsvik, T.H. *et al.* Palaeomagnetism of the Malani Igneous Suite (NW India). *Precambrian Res.* **108**, 319-333 (2001)
10. Gregory, L.C., Meert, J.G., Bingen, B., Pandit, M. & Torsvik, T.H. Paleomagnetism and geochronology of the Malani Igneous Suite, Northwest India: Implications for the configuration of Rodinia and the assembly of Gondwana. *Precambrian Research* **170**, 13-26 (2009).
11. Torsvik, T.H., Ashwal, L.D., Tucker, R.D. & Eide, E.A. Neoproterozoic geochronology and palaeogeography of the Seychelles microcontinent. *Precambrian Research* **110**, 47-59 (2001).
12. Parker, R.L. Rapid calculation of potential anomalies. *Geophys. J. R. Astron. Soc.* **31**, 447-455 (1972).
13. Greenhalgh, E.E. & Kuszniir, N.J. Evidence for thin oceanic crust on the extinct Aegir Ridge, Norwegian Basin, NE Atlantic derived from satellite gravity inversion. *Geophys. Res. Lett.* **34**, L06305 (2007).

14. Chappell, A.R. & Kusznir, N.J. Three-dimensional gravity inversion for Moho depth at rifted continental margins incorporating a lithosphere thermal gravity anomaly correction. *Geophys. J. Intern.* **174**, 1-13 (2008).
15. Sandwell, D.T. & Smith, W.H.F. Global marine gravity from retracked Geosat and ERS-1 altimetry: Ridge segmentation versus spreading rate. *J. Geophys. Res.* **114**, B01411 (2009).
16. Amante, C. & Eakins, B.W. ETOPO1, 1 Arc-Minute Global Relief Model: Procedures, Data Sources and Analysis. *NOAA Technical Memorandum NESDIS NGDC-24*, 19 pp. (2009).
17. Laske, G. & Masters, G. A Global Digital Map of Sediment Thickness. *EOS Trans. AGU*, **78**, F483 (1997).
18. White, R. & McKenzie, D.. Magmatism at rift zones - The generation of volcanic continental margins and flood basalts. *J. Geophys. Res.* **94**, 7685-7729 (1989).
19. McKenzie, D. Some remarks on development of sedimentary basins. *Earth Planet. Sci. Lett.* **40**, 25-32 (1978).
20. Müller, R.D., Sdrolias, M., Gaina, C. & Roest, W.R. Age, spreading rates, and spreading asymmetry of the world's ocean crust. *Geochem. Geophys. Geosyst.* **9**, Q04006 (2008).
21. Smith, R.A. A uniqueness theorem concerning gravity fields. *Proc. Cambridge Phil. Soc.* **57**, 865-870 (1961)
22. Poudjom Djomani, Y.H., O'Reilly, S.Y., Griffin, W.L. & Morgan, P. The density of the subcontinental lithosphere through time. *Earth planet Sci. Lett.*, **184**, 605–621 (2001).
23. Carlson, R.L. & Herrick, C.N. Densities and porosities in the oceanic crust and their variations with depth and age. *J. geophys. Res.* **95**, 9153–9170 (1990).
24. Christensen, N.I. & Mooney, W.D. Seismic velocity structure and composition of the continental crust: a global view. *J. geophys. Res.* **100**, 9761–9788 (1995).
25. Collier, J.S. *et al.* Factors influencing magmatism during continental breakup: New insights from a wide-angle seismic experiment across the conjugate Seychelles-Indian margins, *J. Geophys. Res.* **114**, B03101 (2009).
26. Matthews, K., Müller, R. D, Wessel, P. & Whittaker, J. The tectonic fabric of the ocean basins. *J. Geophysical Res.* **116**, B12109 (2011).
27. Schneider, D.A. & Kent, D.V. In *Proceedings of the Ocean Drilling Program, Scientific Results 115* (Eds Duncan, R.A., Backman, J. & Peterson, L.C.), 717-736 (1990).
28. Vandamme, D. & Courtillot, V. In *Proceedings of the Ocean Drilling Program, Scientific Results 115* (Eds Duncan, R.A., Backman, J. & Peterson, L.C.), 111-117 (1990).

29. Paul, D., White, W.M. & Blichert-Toft, J. Geochemistry of Mauritius and the origin of rejuvenescent volcanism on oceanic island volcanoes. *Geochem. Geophys. Geosyst.* **6**, Q06007 (2005).
30. White, W.M., Cheatham, M.M. & Duncan, R.A. In *Proceedings of the Ocean Drilling Program Scientific results 115* (eds Duncan, R.A., Backman, J. & Peterson, L.C.) 53-61 (1990).
31. Vlastelic, I., Lewin, E. & Staudacher, T. Th/U and other geochemical evidence for the Réunion plume sampling a less differentiated mantle domain. *Earth Planet. Sci. Lett.* **248**, 379-393 (2006).
32. Moore, J. *et al.* Evolution of shield-building and rejuvenescent volcanism of Mauritius. *J. Volc. Geothermal Res.* **207**, 47-66 (2011).
33. Bosch, D. *et al.* Pb, Hf and Nd isotope compositions of two Réunion volcanoes (Indian Ocean): A tale of two small-scale mantle blobs? *Earth Planet. Sci. Lett.* **265**, 748-768 (2008).
34. Fisk, M.R., Upton, B.G.J., Ford, C.E. & White, W.M. Geochemical and experimental study of the genesis of magmas of Réunion island, Indian Ocean. *J. Geophys. Res.* **B93**, 4933-4950 (1988).
35. Fretzdorff, S. & Haase, K.M. Geochemistry and petrology of lavas from the submarine flanks of Réunion Island (Western Indian Ocean): Implications for magma genesis and the mantle source. *Mineral. Petrol.* **75**, 153-184 (2002).
36. Hamlin, B., Dupre, B. & Allegre, C.-J. Pb-Sr-Nd isotopic data of Indian Ocean ridges: New evidence of large-scale mapping of mantle heterogeneities. *Earth Planet. Sci. Lett.* **76**, 288-298 (1985).
37. Mahoney, J.J. *et al.* Isotopic and chemical provinces of the Western Indian Ocean spreading centers. *J. Geophys. Res.* **B94**, 4033-4052 (1989).
38. Newsom, H.E., White, W.M., Jochum, K.P. & Hofmann, A.W. Siderophile and chalcophile element abundances in oceanic basalts, Pb isotope evolution and growth of the Earth's core. *Earth Planet. Sci. Lett.* **80**, 299-313 (1986).
39. Nohda, S., Kaneokai, I., Hanyu Takeshi, XU. S., Uto, K. Systematic variation of Sr-, Nd- and Pb- isotopes with time in lavas of Mauritius, Réunion hot spot. *J. Petrol.* **46**, 505-522 (2005).
40. Luais, B. Temporal changes in Nd isotopic composition of Piton De La Fournaise magmatism (Réunion island, Indian Ocean). *Geochemistry Geophysics Geosystems* **5**, Q01008 (2004).
41. Peng, Z.X., Mahoney, J.J. Drillehole lavas from the northwestern Deccan Traps, and the evolution of Réunion hotspot mantle. *Earth Planet. Sci. Lett.* **134**, 169-185 (1995).
42. Sheth, H.C., Mahoney, J.J. & Baxter, A.N. Geochemistry of lavas from Mauritius, Indian Ocean. *Int. Geol. Rev.* **45**, 780-797 (2003).

43. Tatsumi, Y. & Nohda, S. In *Proceedings of the Ocean Drilling Program, Scientific Results 115* (Eds Duncan, R.A., Backman, J. & Peterson, L.C.), 63-69 (1990).
44. Becker, T.W., Boschi, L. A comparison of tomographic and geodynamic mantle models. *Geochem. Geophys. Geosyst.* **3**, 1003 (2002).
45. Jaffey, A.H., Flynn, K.F., Glendenin, L.E., Bentley, W.C. & Essling, A.M. Precision measurement of half-lives and specific of  $^{235}\text{U}$  and  $^{238}\text{U}$ . *Phys. Rev., Sect. C, Nucl. Phys.* **4**, 1889-1906 (1971).
46. Corfu, F. U–Pb age, setting, and tectonic significance of the anorthosite–mangerite–charnockite–granite-suite, Lofoten–Vesterålen, Norway. *J. Petrol.* **45**, 1799-1819 (2004).